

The optical microvariability and spectral changes of the BL Lacertae object S5 0716+714

H. Poon

Astronomy Department, Beijing Normal University, Beijing 100875, China

china_108@yahoo.com

J. H. Fan

Center for Astrophysics, Guangzhou University, Guangzhou 510006, China

and

J. N. Fu

Astronomy Department, Beijing Normal University, Beijing 100875, China

Received _____; accepted _____

ABSTRACT

We monitored the BL Lac object S5 0716+714 in the optical band during October 2008, December 2008 and February 2009 with a best temporal resolution of about 5 minutes in the *BVRI* bands. Four fast flares were observed with amplitudes ranging from 0.3 to 0.75 mag. The source remained active during the whole monitoring campaign, showing microvariability in all days except for one. The overall variability amplitudes are $\Delta B \sim 0^m.89$, $\Delta V \sim 0^m.80$, $\Delta R \sim 0^m.73$ and $\Delta I \sim 0^m.51$. Typical timescales of microvariability range from 2 to 8 hours. The overall *V - R* color index ranges from 0.37 to 0.59. Strong bluer-when-brighter chromatism was found on internight timescales. However, different spectral behavior was found on intranight timescales. A possible time lag of ~ 11 mins between *B* and *I* bands was found on one night. The shock-in-jet model and geometric effects can be applied to explain the source's intranight behavior.

Subject headings: galaxies: active - BL Lacertae objects: individual: S5 0716+714 - galaxies: photometry

1. Introduction

Blazars represent an extreme subclass of active galactic nuclei. They are characterized by rapid and strong variability throughout the entire electromagnetic wavebands, high and variable polarization ($>3\%$) from radio to optical wavelengths. In the unified model of AGNs, blazars make an angle of less than 10° from the line of sight (Urry & Padovani 1995). For low-energy peaked (or radio-selected) blazars the continuum from radio through the UV or soft X-rays is mainly contributed by synchrotron radiation, while a second hump in the spectrum at higher energies usually peaks in the GeV γ -ray band. Blazars exhibit variability on different timescales, from years down to hours or less (See Fan et al. 2005). Understanding blazar variability is one of the major issues of active galactic nuclei studies. There may be different behavior on different timescales. Periodicity may be found on the long term, as is the case of OJ 287 (Sillanpaa et al. 1988) and other blazars (Fan et al. 2002, 2007). The periodicity of OJ 287 can be explained by a binary black hole model, with the secondary black hole passing through the accretion disk of the primary black hole twice per revolution (Sillanpaa et al. 1988; Lehto & Valtonen 1996). On shorter timescales, 3C 66A was claimed to have an optical period of ~ 65 days during its bright state (Lainela et al. 1999), while Mkn 501 may have displayed a period of 23 days in high energy data (Osone 2006). Recently, analyses of X-ray data have yielded excellent evidence for a quasi-period of about an hour for 3C 273 (Espaillat et al. 2008) and very good evidence for near periods of ~ 16 days for AO 0235+164 and ~ 420 days for 1ES 2321+419 (Rani et al. 2009). This may be due to a shock wave moving along a helical path in the relativistic jet (e.g., Marscher 1996) or the unstability in the accretion disk (Fan et al. 2008) for Mkn 501. Different viewing angles may also result in different level of brightness, with the source being dimmer at larger viewing angles. BL Lacertae shows variability on both intranight and internight timescales with different spectral behaviors. It shows an intranight strongly chromatic trend and an internight mildly chromatic trend,

indicating two different components operating in the engine (Villata et al. 2004; Hu et al. 2006). Understanding the shortest variability timescale is of special importance. Brightness changes of up to a few tenths of a magnitude over the course of a night or less is known as intra-night optical variability (INOV) (Wagner & Witzel 1995) or the so-called microvariability. It can bring new insight into the understanding of the nature of blazars, probing into the innermost structure down to microparsecs, putting constraints on the size of the source and its physical environments.

Microvariability was first discovered in the sixties by Matthews and Sandage (1963), who found 3C 48 changed $0^m.04$ in the V band in 15 minutes. But their results were not taken seriously and were considered due to instrumental errors. However, with the development of CCD, microvariability was confirmed to be the intrinsic nature of active galactic nuclei, especially for blazars (e.g., Miller et al. 1989). From a complete sample of BL Lac objects (Stickel et al. 1991), Heidt and Wagner (1996) found 80% exhibited microvariability, proving it to be the nature of BL Lac objects. Romero et al. (1999) detected microvariability in 60% of their selected sample of 23 southern AGNs. Microvariability became extensively observed since the eighties. Up to now, the reasons for it are still unclear. Many different models have been proposed to explain this phenomenon. It conceivably may be due to eclipses if there is a binary black hole system (Xie et al. 2002). The interaction of relativistic shock waves and inhomogeneous jet can also cause microvariability in the jet (Maraschi et al. 1989; Qian et al. 1991; Marscher 1992; Marscher 1996). Other models like instabilities and perturbations in the accretion disk can explain some of the microvariability phenomena (e.g., Mangalam & Wiita 1993; Wiita 1996; Fan et al. 2008). In order to understand the radiation mechanism and the structure of the radiating region, long-term and multiwavelength observations are needed. The BL Lac object S5 0716+714 is one the brightest BL Lac objects noted for its microvariability. Its high duty cycle means that it is always in an active state (Wagner & Witzel 1995). It

has been the target of many monitoring programs (e.g., Wagner et al. 1996; Qian et al. 2001; Raiteri et al. 2003). Montagni et al. (2006) reported the fastest variability rate of 0.1-0.12mag/hr. Five major outbursts have been observed so far, occurring at the beginning of 1995, in late 1997, in the fall of 2001, in March 2004 and at the beginning of 2007 (Raiteri et al. 2003; Foschini et al. 2006; Gupta et al. 2008). These five outbursts indicate a long-term variability timescale of $\sim 3.0 \pm 0.3$ years (e.g., Raiteri et al. 2003). Correlated radio/optical variability has been observed for the source. In a 4-week monitoring program, Quirrenbach et al. (1991) discovered a period change of 1 day to 7 days in both radio and optical bands. Heidt & Wagner (1996) reported a period of 4 days in the optical band while Qian, Tao & Fan (2002) derived a 10-day period from their 5.3 yr optical monitoring. Recently Gupta et al. (2009) have found good evidence for quasi-periods in five of the 20 best quality nightly data sets of Montagni et al. (2006); these ranged from ~ 23 to ~ 75 minutes.

The spectral change of S5 0716+714 has been observed extensively (e.g., Ghisellini et al. 1997; Raiteri et al. 2003; Villata et al. 2004; Gu et al. 2006; Wu et al. 2005). Different behaviors have been reported. Raiteri et al. (2003) reported different chromatism in different timescales in their 8-year monitoring program. Sometimes the source was bluer when brighter, sometimes the opposite, sometimes no spectral change was seen despite changes in brightness. Ghisellini et al. (1997) and Wu et al. (2005) found the source exhibited a bluer-when-brighter chromatism when it was in fast flares. However, Stalin et al. (2006) found even if the source was in fast flare, there was no color change with brightness. In this paper we concentrate on the microvariability and spectral changes of S5 0716+714. We monitored the source from October 25 to 30 2008, December 23 to 29 2008 and February 3 to 10 2009. The temporal resolution was around 5 to 8 minutes in the four optical bands (*BVRI*). Because of the high temporal resolution, we can provide high quality data with accurate results.

The paper is organized as follows: Section 2 describes observations and data reduction procedures. Section 3 presents the results. Discussions are reported in Section 4. A summary is given in Section 5.

2. Observations and Data Reductions

Our photometric observations were carried out at the 85-cm telescope which is located at the Xinglong Station of the National Astronomical Observatories of China (NAOC). This telescope is equipped with a standard Johnson-Cousin-Bessel multicolor CCD photometric system built on the primary focus (Zhou et al. 2008). The PI1024 BFT camera has 1024×1024 square pixels, a field of view of $16'.5 \times 16'.5$ at a focal ratio of 3.27 ($f = 2780\text{mm}$) with a scale of 0.96 arcsec per pixel.

After flat-fielding, bias and dark corrections, aperture photometry was performed using the `apphot` task of IRAF. The instrumental magnitudes of the source and comparison stars were then collected and then processed in order to obtain the standard magnitudes of S5 0716+71 and the relevant errors (Note that data in the I band were not calibrated due to large photometric errors). Two standard stars in the blazar field, 5 and 6 in the finding chart of Villata et al. (1988), were compared to check that any reported variations were intrinsic to the blazar and that each standard star was non-variable. The magnitude difference between the two stars in the B , V , R , I bands are $0^m.09$, $0^m.08$, $0^m.08$ and $0^m.12$ respectively. The observational log is presented in Tables 1 – 4 with columns being Julian date, magnitude and uncertainty. We first determined the differential instrumental magnitude of the blazar, star 5 and star 6. We determined observational scatter from the blazar – star 5 (σ (BL – Star 5)) and star 5 – star 6 (σ (Star 5 – Star 6)). The rms errors are calculated from the two stars using the formula:

$$\sigma = \sqrt{\frac{\sum(m_i - \bar{m})^2}{N - 1}} \quad (1)$$

where $m_i = (m_5 - m_6)_i$ is the differential magnitude of stars 5 and 6 while $\bar{m} = m_5 - m_6$ is the differential magnitude averaged over the entire dataset, and N is the number of observations on a given night. The variability of the source is then investigated by means of the variability parameter, C , introduced by Romero et al. (1999). This parameter is defined as: $C = \frac{\sigma_{(BL-5)}}{\sigma_{(5-6)}}$. If $C > 2.576$, the source is variable at 99% confidence level. The object is decided to be variable only when $C \geq 2.576$ at least in two bands if it is monitored in three or more bands (Jang & Miller 1997). The intranight variability is calculated (Heidt & Wagner 1996):

$$Amp = \sqrt{(A_{max} - A_{min})^2 - 2\sigma^2}, \quad (2)$$

where A_{max} and A_{min} are the maximum and minimum values of each light curve and σ is the same as what is described above. The results are given in Table 5 for filters B , V , R and I . Column (1) is the universal date of observation, column (2) the band, column (3) the intranight variability amplitude, column (4) the number of data points, column (5) the value of the C parameter (V/N indicates whether the source is variable or not), column (6) the rms errors, column (7) the Pearson correlation coefficients of the $V - R$ color index vs. R magnitude.

Our monitoring program of S5 0716+714 was divided into three periods. The first period was from October 25 to 30 2008, the second from December 23 to 29 2008 and the third from February 3 to 10 2009. As a result of weather conditions, 14 nights of data were obtained. In the first period of our observations, only filters V and R were used. In the second and third periods longer observation times allowed us to usually use four filters: B , V , R and I . The typical exposure times for $BVRI$ measurements were 100s, 70s, 50s and 30s respectively. The readout time is about 10s, resulting in a temporal resolution of around 5 minutes for the best weather conditions. Because of the dense sampling and high quality

(photometric error ~ 0.004 mag), the data set can provide highly reliable results.

3. Results

3.1. Light Curves

The overall light curves in bands V and R are displayed in Fig. 1. The light curves of the two bands for individual periods are displayed in Fig. 2 - 4. The source remained active during the whole period of monitoring. The variations in $BVRI$ are $\Delta B \sim 0^m.89$, $\Delta V \sim 0^m.80$, $\Delta R \sim 0^m.73$ mag, $\Delta I \sim 0^m.51$. One can see four flares during our period of observation for four months (from JD 2454765 to JD 2454873) from Fig. 1. The first flare peaked on JD 2454766, with $V \sim 13^m.41 \pm 0^m.01$, $R \sim 13^m.01 \pm 0^m.01$. It is quite likely that the actual peak was even higher since the blazar's brightness was declining monotonically throughout the period observed that night. After that, the magnitude dropped about 0.4 mag in 4 days. In the second flare, the source brightness rose since the first day (JD 2454824) of our second period of observation, reaching a maximum on JD 2454825 ($V \sim 13^m.59 \pm 0^m.01$, $R \sim 13^m.16 \pm 0^m.01$) and then quickly dropped about 0.5 mag in the following 3 days, reaching a minimum on JD 2454828 ($V \sim 14^m.11 \pm 0^m.04$, $R \sim 13^m.65 \pm 0^m.03$). The source brightness then rose again until the end of our second period of observation, resulting in another flare with a magnitude change of about 0.3 mag in 2 days. In the third period of observations the fourth flare showed the source reaching the maximum brightness seen in our entire data set, with $R \sim 12^m.95 \pm 0^m.01$ and $V \sim 13^m.35 \pm 0^m.01$ on JD 2454867. The source then rapidly dropped about 0.8 mag in 6 days until the end of our observation on JD 2454873.

Clear intranight variations can be seen during the whole monitoring campaign. We detected significant brightness changes in a large fraction of nights: only in 1 night (marked

with an asterisk in Table 5) did the source remain stable during the observation time window. The intranight variability amplitude ranges from $\sim 0.04 - 0.28$ mag with a typical duration of a few hours. The lightcurves of microvariability are generally irregular except for the ones of JD 2454825 and JD 2454826 of period 2 which are symmetric, and may show one possible cycle of ~ 8 hr, respectively. In the first period, the source usually displayed microvariability of large amplitude (>0.1 mag). Some examples of the lightcurves are shown in Fig. 5. On JD 2454765, the source brightened gradually by 0.183 ± 0.01 mag in 192 mins in the R band. On the next day, after reaching the peak of the first flare, the brightness of the source began to fall. The magnitude change was 0.157 ± 0.01 mag in 248 mins in the R band. On the last day of period one, which was JD 2454770, the brightness rose 0.116 ± 0.01 mag in 185 mins in the R band.

In the second period of our observations, noticeable microvariability was observed on JD 2454824 and JD 2454825. On the former day, the brightness first dropped 0.110 ± 0.01 mag in 149 mins in the R band and then became somewhat steady (Fig. 6). On JD 2454825, the lightcurves are symmetric. The source first brightened by 0.105 ± 0.008 mag in 259 minutes, reaching the peak of the second flare, and then gradually dropped $0.137 \text{ mag} \pm 0.01$ in 301 minutes (R band, see Fig. 7). The lightcurves on JD 2454826 are sawtooth-like and have sharp turnoffs, showing a complete period. The brightness of the source first dropped 0.054 ± 0.01 mag in 172 mins and then rose 0.07 ± 0.01 mag in 268 mins (R band). It then dropped again with an amplitude of 0.0461 ± 0.01 mag, a timescale of 117 mins, forming a complete cycle (Fig. 8). The lightcurves of JD 2454825 and JD 2454826 are of particular interest and are discussed further in section 4.

In the third period of our observations, the source showed substantial brightness changes in all the four days of observations. On JD 2454865 - 2454866, it first dropped 0.112 ± 0.02 mag in 258 mins and then rose 0.073 ± 0.01 in 206 mins (R band, see Fig. 9).

On 2454866 - 2454867, in the R band, the source brightened steadily by 0.152 ± 0.02 mag in 145 mins, reaching the peak of the fourth flare, and then it dropped 0.07 ± 0.01 mag in 463 mins (Fig. 10). The source displayed the greatest magnitude change on JD 2454871 - 2454872. The brightness dropped 0.245 ± 0.03 mag over the course of the night in 480 mins (R band, see Fig. 11). On the last night of our whole observation campaign, JD 2454872 - 2454873, the source displayed a rather regular lightcurve. At the beginning, the brightness dropped 0.082 ± 0.01 mag in 274 mins and then rose 0.113 ± 0.01 mag in 240 mins (R band, see Fig. 12). From Fig. 5 - 12, one can see the lightcurves of microvariability of different bands are consistent with each other.

3.2. Spectral Variability

Based on our observations of high temporal resolution, the spectral variability with brightness was investigated in this section. Magnitudes have been dereddened by using a galactic extinction coefficient $A_B = 0.132$, $A_V=0.102$, $A_R=0.082$ (Schlegel et al. 1998). We concentrate on the $V-R$ index, the best sampled one. The overall $V - R$ color index ranges from 0.380 to 0.485. For individual nights showing microvariability, the spectral behavior varies from night to night (see Fig. 13). A clear bluer-when-brighter chromatism is evident in the long-term trend. The changes of color index with brightness during the whole monitoring campaign are shown in Fig. 14. The solid line is the unweighted least-squares fit to the data points, which has a slope of 0.02 and a correlation coefficient of 0.753, indicating a strong correlation between color and magnitude. However, the color-magnitude correlation is complex in the three observation periods.

Those nights showing strong correlation between color and magnitude are shown in Fig. 15. In the first period of our observations (JD 2454765 - JD 2454770), the source displayed the strongest bluer-when-brighter (BWB) behavior. Clear microvariability was

observed on all nights, with variability amplitude ranging from $\sim 0.04 - 0.2$ (see Table 5). On the first night of observations of period 1, JD 2454765, the variability amplitude in the R band is 0.183 mag and the correlation coefficient is 0.859. The mean R magnitude was $\sim 13^m.12$. On the next day, the variability amplitude was somewhat smaller, $\Delta R = 0.157$ mag ($\bar{R} \sim 13^m.09$) and the correlation coefficient $r = 0.827$. On JD 2454767, the variability amplitude was the smallest among all days of observations in period 1, $\Delta R = 0.048$ mag ($\bar{R} \sim 13^m.15$) and $r = 0.430$. On JD 2454770, the amplitude is $\Delta R = 0.116$ mag ($\bar{R} \sim 13^m.32$) and $r = 0.749$. One can see a noticeable trend that the source showed a stronger BWB chromatism when the amplitude change became larger in period 1. However, this trend does not seem to be related to brightness. BWB chromatism can be found both when the source was at the brightest state ($\bar{R} \sim 13^m.09$ on JD 2454766) and the dimmest state ($\bar{R} \sim 13^m.32$ on JD 2454770) of period 1.

In the second period of our observations (JD 2454824 - JD 2454830), BWB is still noticeable on the first two nights of observation. The variability amplitude of these two nights were 0.127 and 0.137 mag respectively (R band), the corresponding mean R magnitudes were $\sim 13^m.36$ and $\sim 13^m.21$ and the corresponding correlation coefficients were 0.563 and 0.618. However, on subsequent nights with smaller variability amplitude, an achromatic trend is noticed. On JD 2454826, JD 2454828 and JD 2454829, the amplitude changes in the R band were 0.070, 0.043 and 0.071 mag respectively, the corresponding correlation coefficients r were 0.150, -0.187 and 0.323, indicating no clear relationship between color and brightness. The source was at a rather dim state in these 3 days, with $\bar{R} \sim 13^m.34$ on JD 2454826, $\bar{R} \sim 13^m.50$ on JD 2454828 and $\bar{R} \sim 13^m.40$ on JD 2454829. The trend that the source displayed stronger BWB chromatism with increasing variability amplitude is still noticeable in period 2 but not as obvious as in period 1 and again the color change does not seem to be related to brightness.

In the third period of observations (JD 2454865 - JD 2454873), each night showed a variability magnitude of > 0.1 mag. The source was observed for four nights in this period. It showed an achromatic trend on the first three nights of observations with $\Delta R = 0.112$ ($\bar{R} \sim 13^m.35$) on JD 2454865 - JD 2454866, $\Delta R = 0.152$ ($\bar{R} \sim 12^m.99$, the brightest state in the whole monitoring campaign) on JD 2454866 - JD 2454867 and $\Delta R = 0.245$ ($\bar{R} \sim 13^m.34$) on JD 2454871 - JD 2454872. The corresponding correlation coefficients are -0.198 , 0.333 and 0.115 respectively, indicating no clear correlation between color and brightness. However, on JD 2454873, the source was at the dimmest state in the whole monitoring campaign with $\bar{R} \sim 13^m.64$ and $\Delta R = 0.113$, a BWB trend is noticeable with correlation coefficient $r = 0.516$. Very obviously spectral change is neither related to brightness nor variability amplitude in period 3.

On the whole, we find no consistent relation between color vs magnitude and also color vs variability amplitude on intranight timescale. BWB chromatism and achromatism can be found when the source is bright or faint, showing large variability amplitude or small variability amplitude. This suggests that even on intranight timescales, different mechanisms may be at work.

4. Discussions

The microvariability of S5 0716 + 714 has been observed by many authors. Some ultra-rapid fluctuations on timescale ≤ 1.0 hour were reported. Qian et al. (2002) recorded a brightness increase of $\Delta V \sim 0.78$ mag in 9 mins in their 5.3-yr monitoring programme. Xie et al. (2004) reported $\Delta B \sim 0.55$ mag on a timescale of 36 mins. On longer timescales, Gu et al. (2006) found the magnitude change of $\Delta V = 0.28$ mag in ~ 5 hours. In our monitoring programme, no ultra-rapid fluctuations were detected. The shortest timescale was ~ 2 hours, corresponding to $\Delta R \sim 0.046$ mag on JD 2454826 while the longest timescale

were ~ 8 hours, corresponding to $\Delta R \sim 0.245$ mag, which happened on JD 2454871 - JD 2454872. In our whole monitoring campaign, the timescales are generally a few hours with amplitude of $\sim 0.04 - 0.28$ mag.

Time lags between different optical bands have also been reported. Stalin et al. (2006) found possible time lags of ~ 6 and ~ 13 mins between the V and R bands in their 2 nights of observations of the source. Qian et al. (2000) reported similar results in which they found a time lag of ~ 6 mins between the V and I bands. From densely sampling data, Villata et al. (2000) presented a time lag with a strict upper limit of ~ 10 mins between the B and I band. In this work, we tried to find out the time lag between B band and I band using the discrete cross-correlation function, DCF, suggested by Edelson & Krolik (1988) for unequally spaced data. It was performed only on the day with high-quality data (error ~ 0.003 and ~ 0.005 for B and I band respectively) and dense sampling rate (temporal resolution ~ 5 minutes), which is JD 2454826, the day with with a hint of periodicity in its light curve. Fig. 16 presents the results of the calculations. The dashed line indicates the centroid which was calculated using the method proposed by Peterson (2001) and we found the barycenter using data points located near the peak value, DCF_{peak} , specifically, those greater than $0.8DCF_{peak}$. The expression is:

$$DCF_{centroid} = \frac{\sum \tau DCF(\tau)}{\sum DCF(\tau)} \quad (3)$$

We found a time lag of ~ 11 minutes, with the B band leading I band. However, given the sampling rate of ~ 5 minutes and the negligible difference between the DCF values at -20 minutes and 0 minutes, this cannot be considered a convincing measurement of a lag. This result is consistent with Villata et al. (2000), who presented a strict upper limit of ~ 10 minutes to a possible delay between B - and I - band variations using high-quality, densely sampled data on a single night. This result is expected in the shock-in-jet model but not in most disc-based variability models (e.g. Wiita 2006).

In order to quantitatively analyze possible periods, we performed structure function (SF) on JD 2454826, the only day with a lightcurve that shows a hint of a period. SF, discussed fully by Simonetti et al. (1985), is a common tool to search for periodicities and timescales of variation. It identified a timescale of 259 mins, 287 mins, 280 mins and 263 mins and a period of 482 mins, 497 mins, 498 mins and 491 mins were found for B , V , R and I band respectively. All these results are consistent with visual inspection. The results are shown in Fig. 17. Of course, since only one “cycle” is present that night, the presence of a period is no more than speculative; such a possible period does not appear to extend to the previous night, for which there is also data. Only observations made with multiple ground based telescopes at different longitudes (or space based telescopes) can convincingly find intranight periods that substantially exceed ~ 1 hr.

The spectral variability of blazars has been investigated by many authors (e.g., Ghisellini et al. 1997; Fan & Lin 1999; Romero et al. 2000; Raiteri et al. 2003; Villata et al. 2000, 2004). Raiteri et al. (2003) found different spectral behavior for the S5 0716 + 714 in short timescales. Sometimes the source was bluer when brighter, sometimes the opposite and sometimes no spectral change was seen. Stalin et al. (2006) found no clear evidence of color variation with brightness in either their internight or intranight monitoring of the source for a fortnight. Ghisellini et al. (1997) and Wu et al. (2005) reported a BWB trend during fast flares but this trend is insensitive in the long-term. However, Wu et al. (2007) noticed that the source is bluer when brighter on both intranight and internight timescales but this trend was not present in the long-term data.

In our monitoring campaign, the source also showed different spectral change behavior. On the long term, the source showed a bluer-when-brighter behavior. Unlike previous studies which reported consistent trends on spectral behavior on intranight timescales (e.g. Ghisellini et al. 1997, Stalin et al. 2006, Wu et al. 2005), no consistent spectral behavior is

found among all those nights displaying microvariability in our present study. The source displayed BWB chromatism when it was either bright or dim, or when showing large or small variability amplitudes. Achromatism was also found when the source was in the same conditions, suggesting different mechanisms for microvariability. The BWB behavior is consistent with shock-in-jet model (Wagner et al. 1995). In this model, shocks form at the base of the jet and propagate downstream, accelerating electrons and compressing magnetic fields and resulting in the observed variability. The model predicts a BWB phenomenon and an irregular lightcurve, as observed in our cases showing this phenomenon. In the case of JD 2454825 and JD 2454826, a symmetric lightcurve was observed for the former case while a periodic lightcurve for the latter. Such regular lightcurves are rarely found. Wu et al. (2005) reported a single “period” of a sine-like light curve on intranight timescales for two nights during their observations of S5 0716+714. Using more sophisticated techniques Gutpa et al. (2009) found multiple oscillations to be present during 5 nights out of the 20 highest quality light curves of a total sample of 102 nights of data by Montagni et al. (2006). Unlike ours, their lightcurves are sinelike with smooth turns while ours are sawtooth-like with sharp turnoffs. The symmetric lightcurves on JD 2454825 showed a correlation between color and magnitude, with the correlation coefficient $r = 0.616$. So the variation may still be due to intrinsic reasons. However, for the periodic lightcurve on JD 2454826, no strong correlation between color and magnitude is found, with the correlation coefficient $r = 0.150$. Such achromatic lightcurves may be produced by geometric effects like microlensing or a lighthouse effect produced by different amounts of Doppler boosting induced by a helical structure to the jet (e.g. Wagner & Witzel 1995). Microlensing predicts a strictly symmetric lightcurve, which cannot explain the concave shape of the second halves of the light curves in our case. Therefore a lighthouse effect is the most probable mechanism for explaining periodic components in blazar lightcurves as this type of variation is likely to be achromatic (e.g., Camenzind & Krockenberger 1992; Gopal-Krishna & Wiita

1992).

5. Summary

We monitored S5 0716+714 during the period October 2008 to February 2009. The object remained active during the whole campaign, showing microvariability on all nights of observations except for one. The timescales range from $\sim 2 - 8$ hours and variability amplitude $\sim 0.04 - 0.28$ mag. Four flares of amplitude of ~ 0.4 mag, 0.5 mag, 0.3 mag and 0.75 mag were observed, each lasting for a few days. The long-term spectral change is evidently bluer-when-brighter. Among those nights displaying microvariability, the source displayed different spectral behavior. Sometimes the source seemed to become bluer with increasing variability amplitude while sometimes not. In a bright state, it displayed a BWB chromatism but this was also found when the source was in a dim state. Achromatism was also observed when the source was both bright and dim. The bluer-when-brighter behavior can be explained by shock-in-jet model while the achromatic trend may be due to geometric effects. A possible time lag of ~ 11 minutes between the B and I bands was seen during one night.

This work is supported by the National Natural Science Foundation of China (NSFC), through the Grants 10673001, 10778601, 10878007 and 10633010 the support from the program for New Century Excellent Talents in University (NCET), and the Project sponsored by the Scientific Research Foundation for the Returned Overseas Chinese Scholars, State Education Ministry.

REFERENCES

- Camenzind, M., & Krockenberger, M. 1992, *A&A*, 255, 59
- Edelson, R. A., & Krolik, J. H. 1988, *ApJ*, 333, 646
- Espallat, C., Bregman, J., Hughes, P., & Lloyd-Davies, E. 2008, *ApJ*, 679, 182
- Fan, J. H., & Lin, R. G. 1999, *ApJS*, 121, 131
- Fan, J. H., Lin, R. G., Xie, G. Z., Zhang, L., Mei, D. C., Su, C. Y., & Peng, Z. M. 2002, *A&A*, 381, 1
- Fan, J. H., Romero, G. E., Wang, Y. X., & Zhang, J. S. 2005, *ChJAA*, 5, 457
- Fan, J. H., et al. 2007, *A&A*, 462, 547
- Fan, J. H., et al. 2008, *APh*, 28, 508
- Foschini, L., et al. 2006, *A&A*, 455, 871
- Ghisellini, G., et al. 1997, *A&A*, 327, 61
- Gopal-Krishna, & Wiita, P. J. 1992, *A&A*, 259, 109
- Gu, M. F., Lee, C. U., Pak, S., Yim, H. S., & Fletcher, A. B. 2006, *A&A*, 450, 39
- Gupta, A. C., Fan, J. H., Bai, J. M., & Wagner, S. J. 2008, *AJ*, 135, 1384
- Gupta A. C., Srivastava A. K., & Wiita P. J. 2009, *ApJ*, 690, 216
- Heidt, J., & Wagner, S. J. 1996, *A&A*, 305, 42
- Hu, S.M., Wu, J. H., Zhao, G., & Zhou, X. 2006, *MNRAS*, 373, 209
- Jang M., & Miller H. R. 1997, *AJ*, 114, 565

- Lainela, M., et al. 1999, ApJ, 521, 561
- Lehto, H. J., & Valtonen, M. J. 1996, ApJ, 460, 207
- Mangalam, A. V., & Wiita, P. J. 1993, ApJ, 406, 420
- Maraschi, L., Celotti, A., & Treves, A. 1989, ESASP, 296, 825
- Marscher, A. P., & Bloom, S. D. 1992, NASA Conf. Pub. 3137, 346, I21
- Marscher, A. P. 1996, ASPC, 110, 248
- Matthews, T. A., & Sandage, A. R. 1963, ApJ, 138, 30
- Miller, H. R., Carini, M. T., & Goodrich, B. D. 1989, Nat, 337, 627
- Montagni, F., Maselli, A., Massaro, E., Nesci, R., Sclavi, S., & Maesano, M. 2006, A&A, 451, 435
- Nesci, R., Massaro, E., & Montagni, F. 2002, PASA, 19, 143
- Osone, S. 2006, APh, 26, 209
- Peterson B.M. 2001, in Advanced Lectures on the Starburst-AGN Connection, eds. I. Aretxaga, D. Kunth and R. Mujica, p3, World Scientific, Singapore
- Qian, S. J., Quirrenbach, A., Witzel, A., Krichbaum, T. P., Hummel, C. A., & Zensus, J. A. 1991, A&A, 241, 15
- Qian, B. C., Tao, J., & Fan, J. H. 2000, PASJ, 52, 1075
- Qian, B., Tao, J., & Fan, J. 2002, AJ, 123, 678
- Quirrenbach, A., et al. 1991, A&A, 372: 71
- Raiteri, C. M., et al. 2003, A&A, 402, 151

- Rani B., Wiita P. J., & Gupta A. 2009, ApJ, 696, 2170
- Romero, G. E., Cellone, S. A., & Combi, J. A. 1999, A&AS, 135, 477
- Romero, G. E., Cellone, S. A., & Combi, J. A. 2000, A&A, 306, L47
- Schlegel, D. J., Finkbeiner, D. P., & Davis, M. 1998, AJ, 500, 525.
- Sillanpaa, A., Haarala, S., Valtonen, M. J., Sundelius, B., & Byrd, G. G. 1988, ApJ, 325, 628
- Simonetti, J. H., Cordes, J. M., & Heeschen, D. S. 1985, ApJ, 296, 46
- Stalin, C., Gopal-Krishn, Sagar, R., Wiita, P. J., Mohan, V., & Pandey, A. K. 2006, MNRAS, 366, 1337
- Stickel, M., Fried, J. W., Kuehr, H., Padovani, P., & Urry, C. M. 1991, ApJ, 374, 431
- Urry, C. M., & Padovani, P. 1995, PASP, 107, 803
- Villata M., Raiteri, C. M., Lanteri, L., Sobrito, G., & Cavallone, M. 1998, A&AS, 130, 305
- Villata M., et al. 2000, A&A, 363, 108
- Villata M., et al. 2004, A&A, 421, 103
- Wagner, S. J., & Witzel, A. 1995, ARA&A, 33, 163
- Wagner, S. J., et al. 1996, AJ, 111, 2187
- Wiita, P. J. 1996, ASPC, 110, 42
- Wiita, P. J. 2006, ASP Conf. Ser. 350, Blazar Variability Workshop II: Entering the GLAST Era, ed. H. R. Miller, K. Marshall, J. R. Webb, M. F. Aller (San Francisco: ASP), 183

Wu, J., Peng, B., Zhou, X., Ma, J., Jiang, Z., & Chen, J. 2005, *AJ*, 129, 1818

Wu, J., Zhou, X., Ma, J., Wu, Z., Jiang, Z., & Chen, J. 2007, *AJ*, 133, 1599

Xie, G. Z., Liang, E. W., Zhou, S. B., Li, K. H., Dai, B. Z., & Ma, L. 2002, *MNRAS*, 334,
459

Zhou, A.Y., Jiang, X. J., Zhang, Y. P., & Wei, J. Y. 2009, *RAA*, 9, 349

Table 1. Observational data for S5 0716+714 (*B* filter)

Julian Date	mag	σ
2454824.05104	14.191	0.010
2454824.05473	14.204	0.010
2454824.05844	14.203	0.009
2454824.06213	14.209	0.009
2454824.06583	14.210	0.009
2454824.06953	14.224	0.009
2454824.07322	14.222	0.009
2454824.07692	14.230	0.011
2454824.08061	14.238	0.010
2454824.08431	14.244	0.013

(This table is available in its entirety in a machine-readable form in the online journal. A portion is shown here for guidance regarding its form and content)

Table 2. Observational data for S5 0716+714 (*V* filter)

Julian Date	mag	σ
2454765.19653	13.600	0.015
2454765.19877	13.605	0.015
2454765.20096	13.604	0.015
2454765.20315	13.615	0.015
2454765.20534	13.613	0.015
2454765.20751	13.611	0.015
2454765.20970	13.614	0.015
2454765.21189	13.617	0.015
2454765.21407	13.615	0.015
2454765.21625	13.617	0.015

(This table is available in its entirety in a machine-readable form in the online journal. A portion is shown here for guidance regarding its form and content)

Table 3. Observational data for S5 0716+714 (*R* filter)

Julian Date	mag	σ
2454765.19751	13.190	0.013
2454765.19987	13.188	0.011
2454765.20206	13.190	0.011
2454765.20424	13.194	0.011
2454765.20642	13.186	0.011
2454765.20861	13.194	0.011
2454765.21080	13.191	0.011
2454765.21297	13.194	0.011
2454765.21516	13.191	0.011
2454765.21735	13.199	0.011

(This table is available in its entirety in a machine-readable form in the online journal. A portion is shown here for guidance regarding its form and content)

Table 4. Observational data for S5 0716+714 (*I* filter)

Julian Date	Differential mag(BL - S ₅)	σ
2454824.05376	-0.004	0.006
2454824.05745	0.005	0.006
2454824.06116	0.000	0.006
2454824.06485	-0.009	0.006
2454824.06855	-0.021	0.006
2454824.07225	-0.020	0.006
2454824.07594	-0.022	0.006
2454824.07964	-0.008	0.006
2454824.08333	-0.001	0.035
2454824.08703	0.012	0.009

(This table is available in its entirety in a machine-readable form in the online journal. A portion is shown here for guidance regarding its form and content)

Table 5. Results of microvariability of the BL Lacertae S5 0716+714

Date (dd.mm.yyyy)	Band	Amplitude (mag)	N	C(V/N)	σ	r
25.10.2008	V	0.200	94	9.03(V)	0.008	0.859
25.10.2008	R	0.183	92	13.90(V)	0.005	...
26.10.2008	V	0.163	82	17.09(V)	0.003	0.827
26.10.2008	R	0.157	84	16.30(V)	0.003	...
27.10.2008	V	0.048	63	4.08(V)	0.003	0.430
27.10.2008	R	0.042	62	4.00(V)	0.003	...
30.10.2008	V	0.133	80	14.24(V)	0.003	0.749
30.10.2008	R	0.116	79	14.55(V)	0.003	...
23.12.2008	B	0.150	107	6.83(V)	0.005	0.563
23.12.2008	V	0.138	107	7.80(V)	0.004	...
23.12.2008	R	0.127	107	7.02(V)	0.004	...
23.12.2008	I	...	107	1.66(N)	0.015	...
24.12.2008	V	0.132	110	15.47(V)	0.003	0.618
24.12.2008	R	0.137	110	14.09(V)	0.003	...
24.12.2008	I	0.139	109	3.88(V)	0.010	...
25.12.2008	B	0.089	127	6.47(V)	0.003	0.150
25.12.2008	V	0.080	128	5.51(V)	0.004	...
25.12.2008	R	0.070	126	4.45(V)	0.004	...
25.12.2008	I	0.074	128	3.51(V)	0.005	...
27.12.2008	B	0.058	36	3.42(V)	0.005	-0.187
27.12.2008	V	0.045	51	2.67(V)	0.006	...

Table 5—Continued

Date (dd.mm.yyyy)	Band	Amplitude (mag)	N	C(V/N)	σ	r
27.12.2008	R	0.043	50	2.68(V)	0.006	...
27.12.2008	I	...	51	2.03(N)	0.008	...
28.12.2008	V	0.069	148	5.14(V)	0.003	0.323
28.12.2008	R	0.071	148	4.36(V)	0.004	...
*29.12.2008	V	...	84	1.98(N)	0.003	...
*29.12.2008	R	...	84	2.17(N)	0.003	...
*29.12.2008	I	...	84	1.61(N)	0.005	...
03.02.2009	V	0.108	178	4.86(V)	0.005	-0.198
03.02.2009	R	0.112	177	5.10(V)	0.005	...
04.02.2009	B	0.181	126	5.42(V)	0.006	0.333
04.02.2009	V	0.157	127	5.42(V)	0.006	...
04.02.2009	R	0.152	127	4.67(V)	0.006	...
04.02.2009	I	...	125	1.97(N)	0.006	...
09.02.2009	B	0.276	102	7.60(V)	0.011	0.115
09.02.2009	V	0.274	100	8.93(V)	0.009	...
09.02.2009	R	0.245	102	6.64(V)	0.011	...
09.02.2009	I	0.225	102	6.46(V)	0.011	...
10.02.2009	B	0.121	86	7.87(V)	0.004	0.516
10.02.2009	V	0.116	86	8.26(V)	0.004	...
10.02.2009	R	0.113	85	8.10(V)	0.004	...

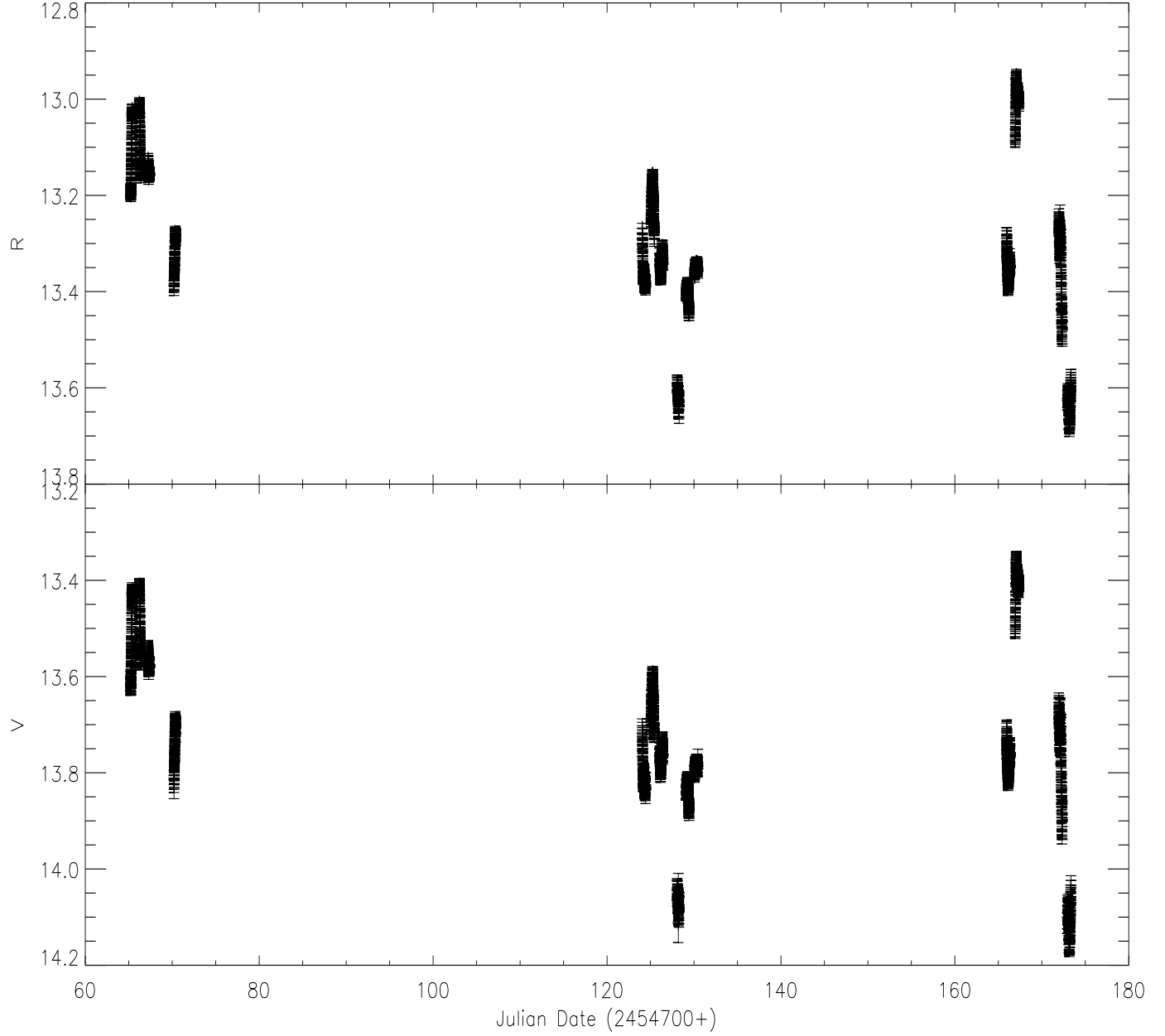


Fig. 1.— Light curves of S5 0716+714 in the VR bands from October 25, 2008 to February 10, 2009.

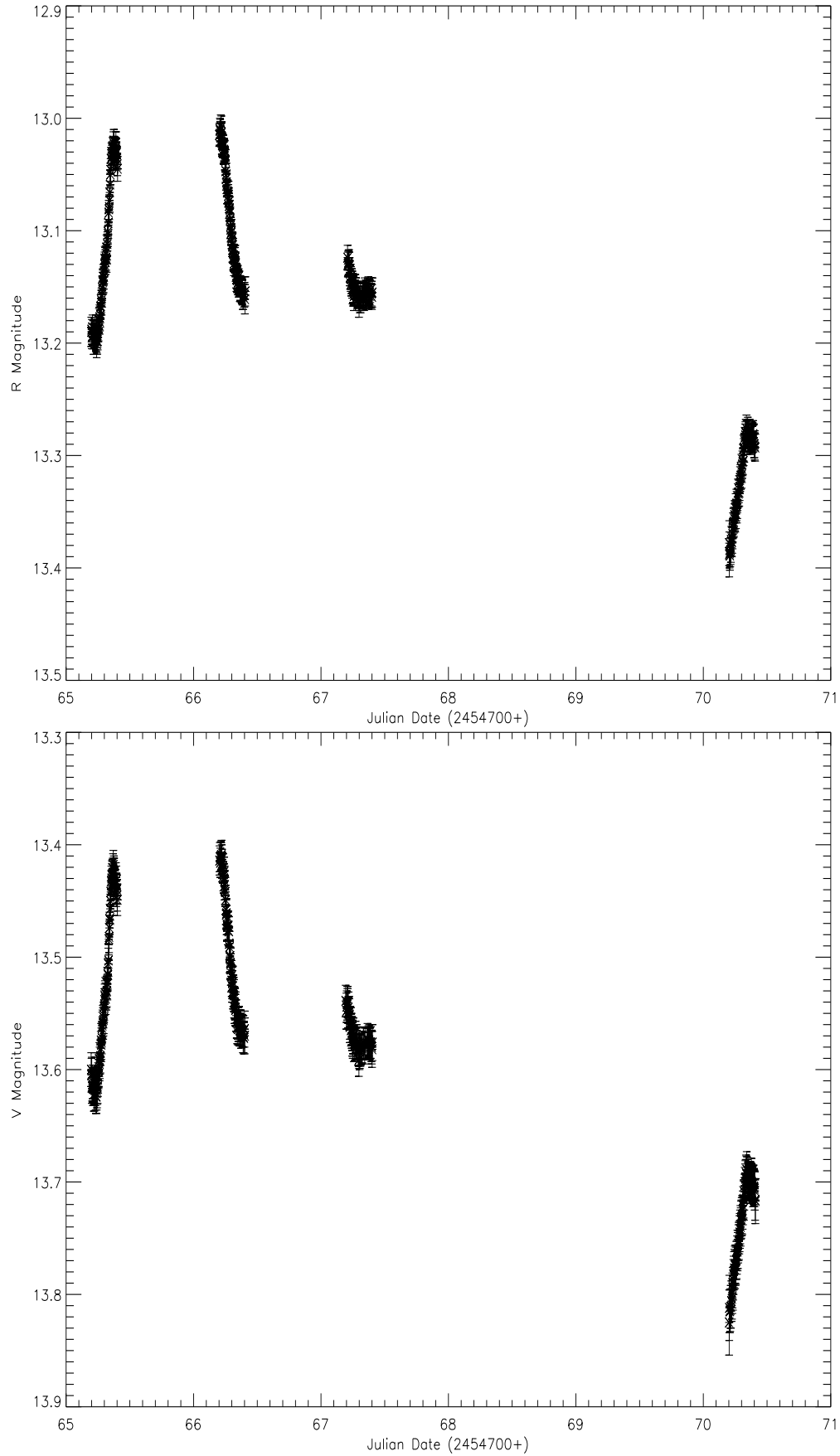


Fig. 9. Light curves of G5 0716+714 in the R ($\lambda_{center} = 640$ nm) and V ($\lambda_{center} = 540$ nm) bands in epoch 1.

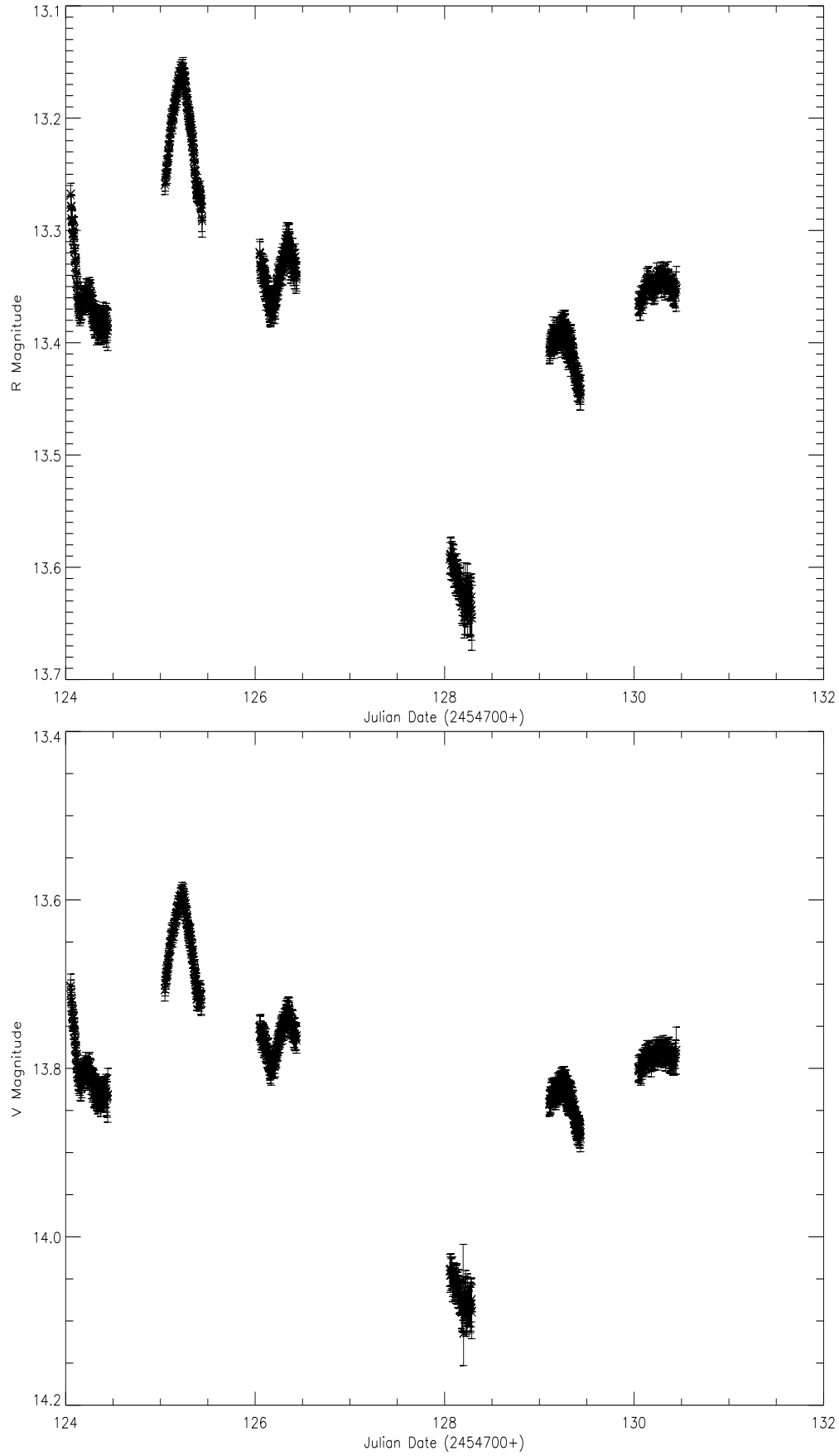


Fig. 2. Light curves of G5 0716+714 in the V ($\lambda_{center} = 5450 \text{ \AA}$) and R ($\lambda_{center} = 6450 \text{ \AA}$) bands in period 19.

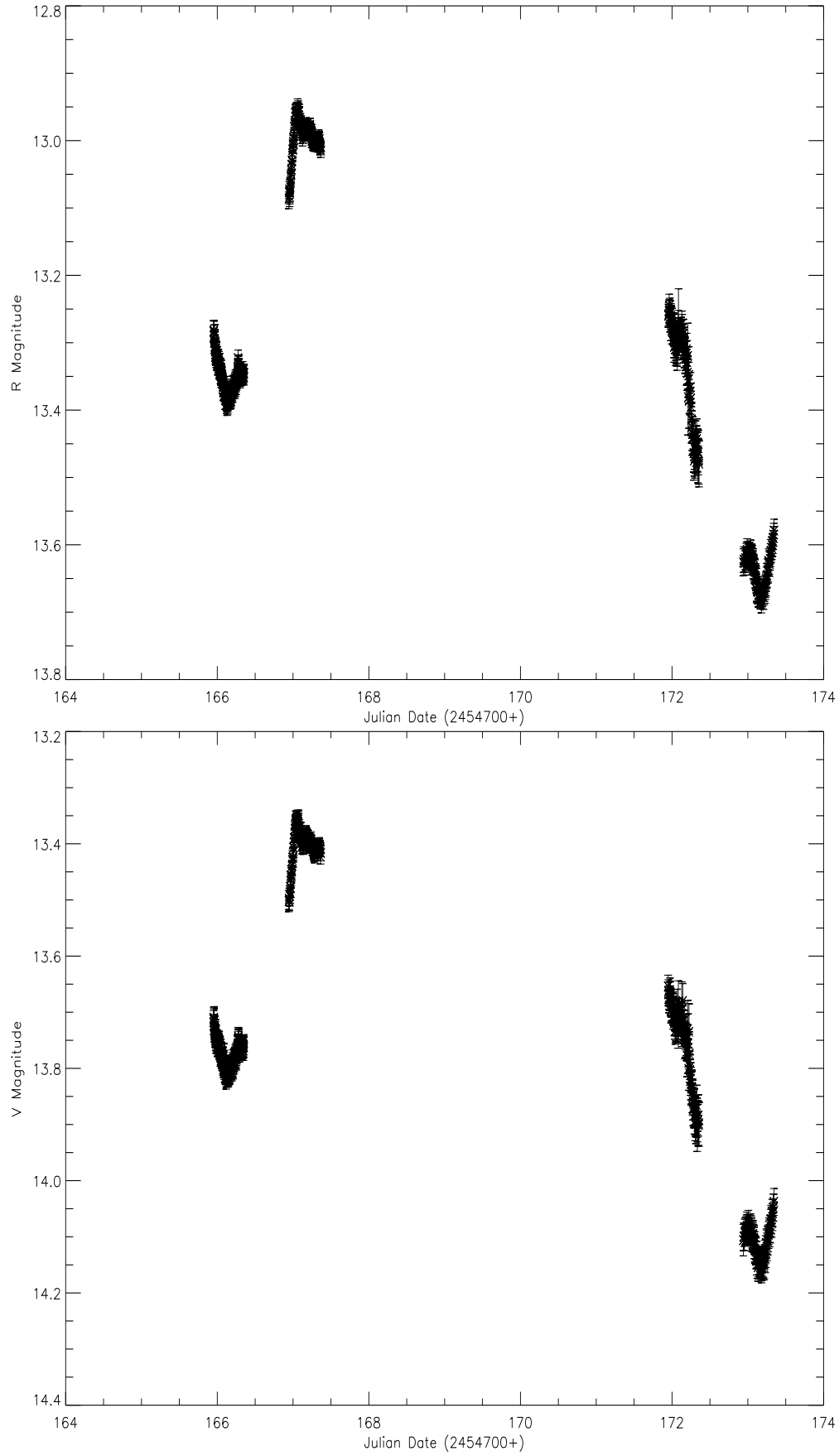


Fig. 4. Light curves of G5 0716+714 in the R (top) and V (bottom) bands in epoch 2.

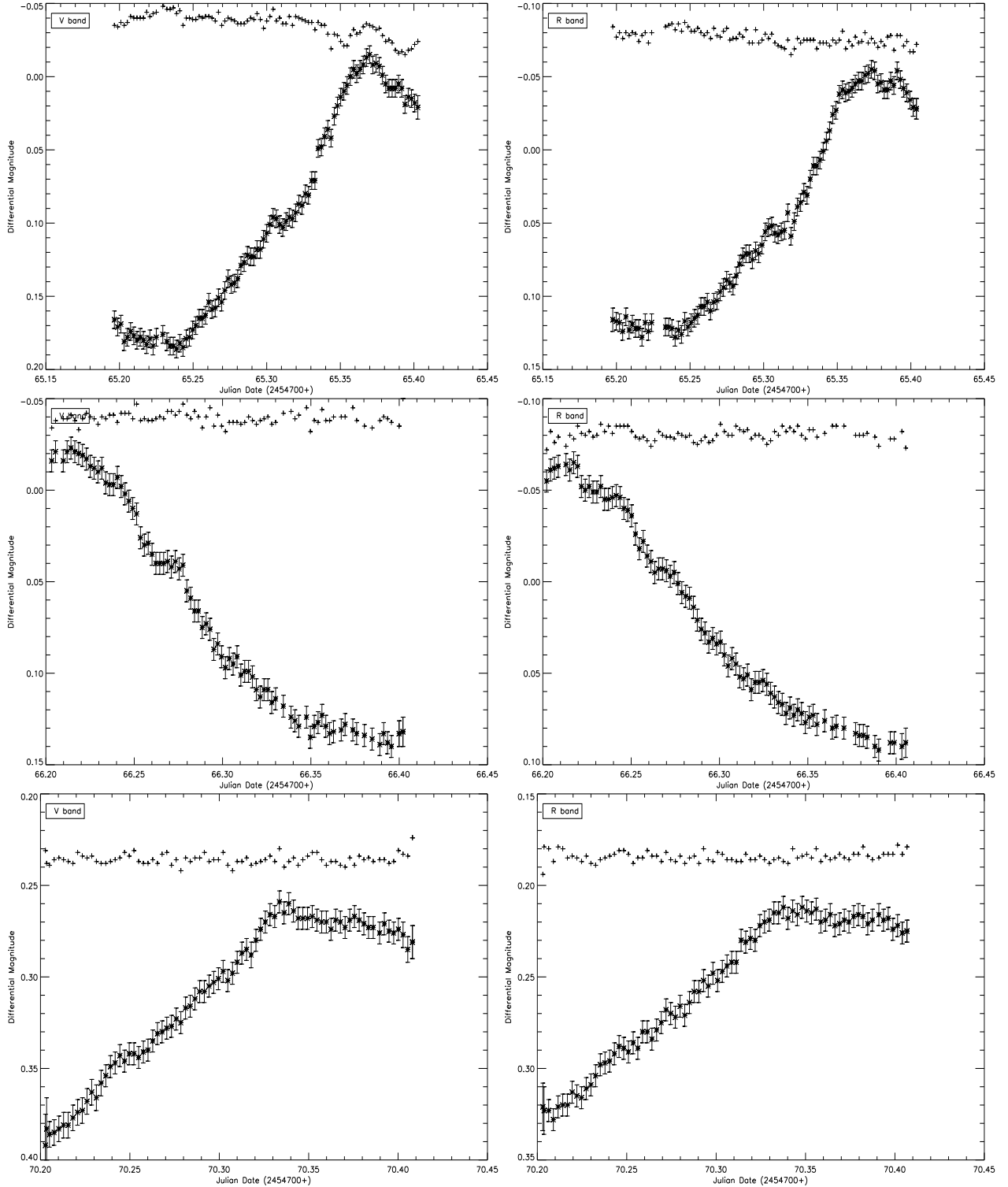


Fig. 5.— Intranight differential light curves of period 1 in V and R bands. The observation date are JD 2454765 (top left for V band and top right for R band), JD 2454766 (middle left for V band and middle right for R band) and JD 2454770 (bottom left for V band and bottom right for R band). Crosses represent the differential magnitude between the source and star 5 while diamonds represent the differential magnitude between star 5 and star 6.

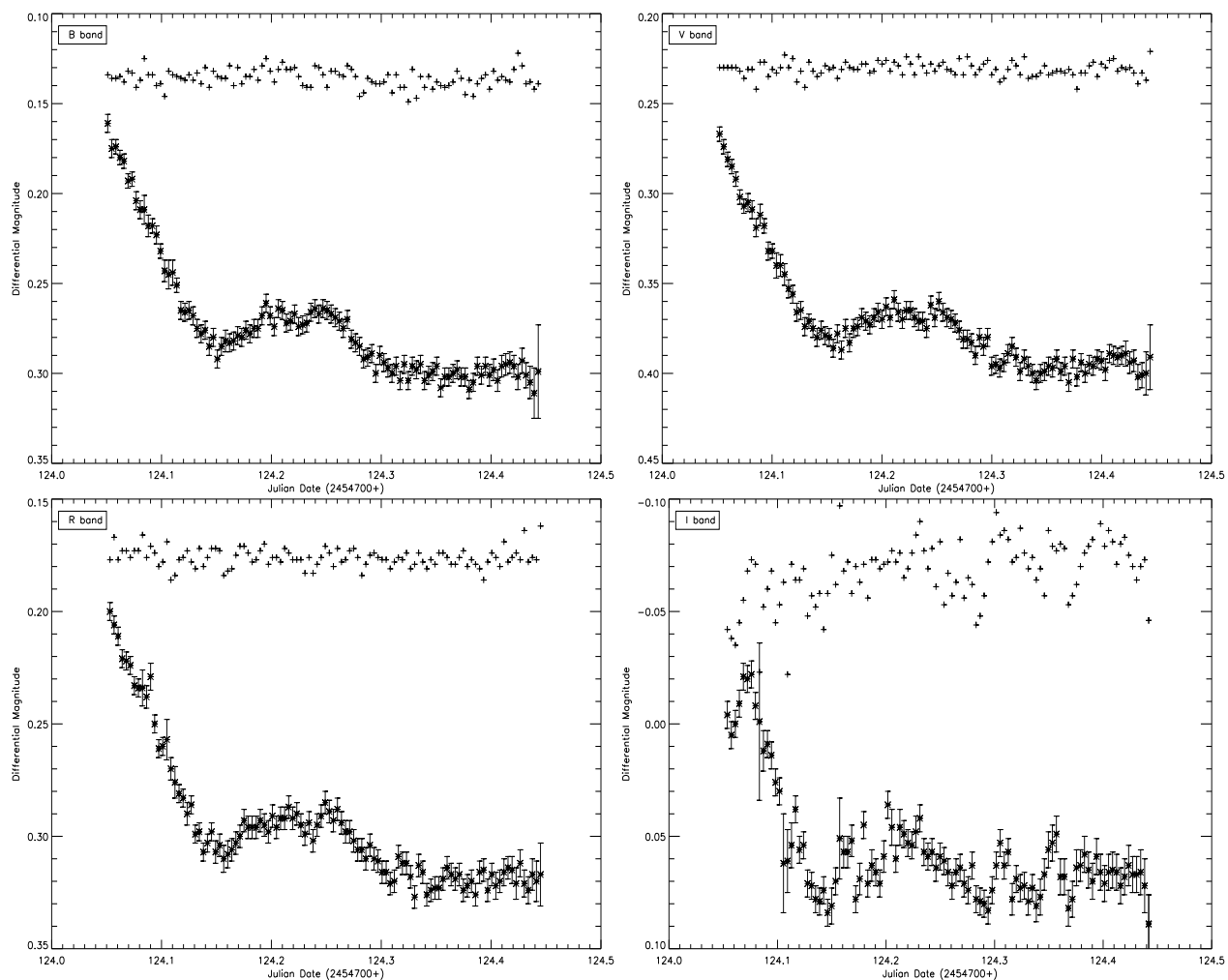


Fig. 6.— Intranight differential light curves on JD 2454824 in B (top left), V (top right), R (bottom left) and R (bottom right) bands. Crosses represent the differential magnitude between the source and star 5 while plus signs represent the differential magnitude between star 5 and star 6 shifted by an arbitrary offset.

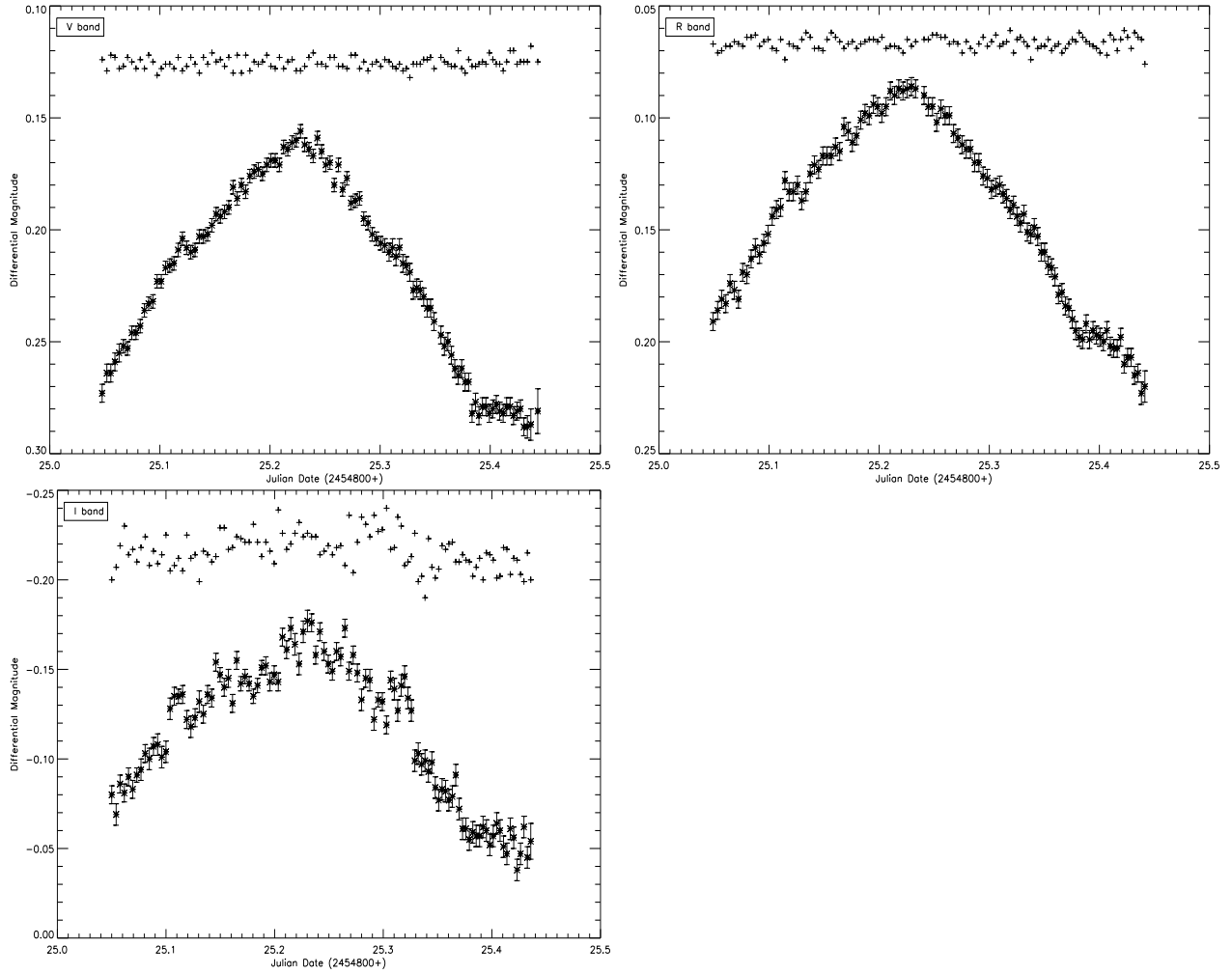


Fig. 7.— Intranight differential light curves on JD 2454825 in V (top left), R (top right) and I (bottom left) bands. Crosses represent the differential magnitude between the source and star 5 while plus signs represent the differential magnitude between star 5 and star 6 shifted by an arbitrary offset.

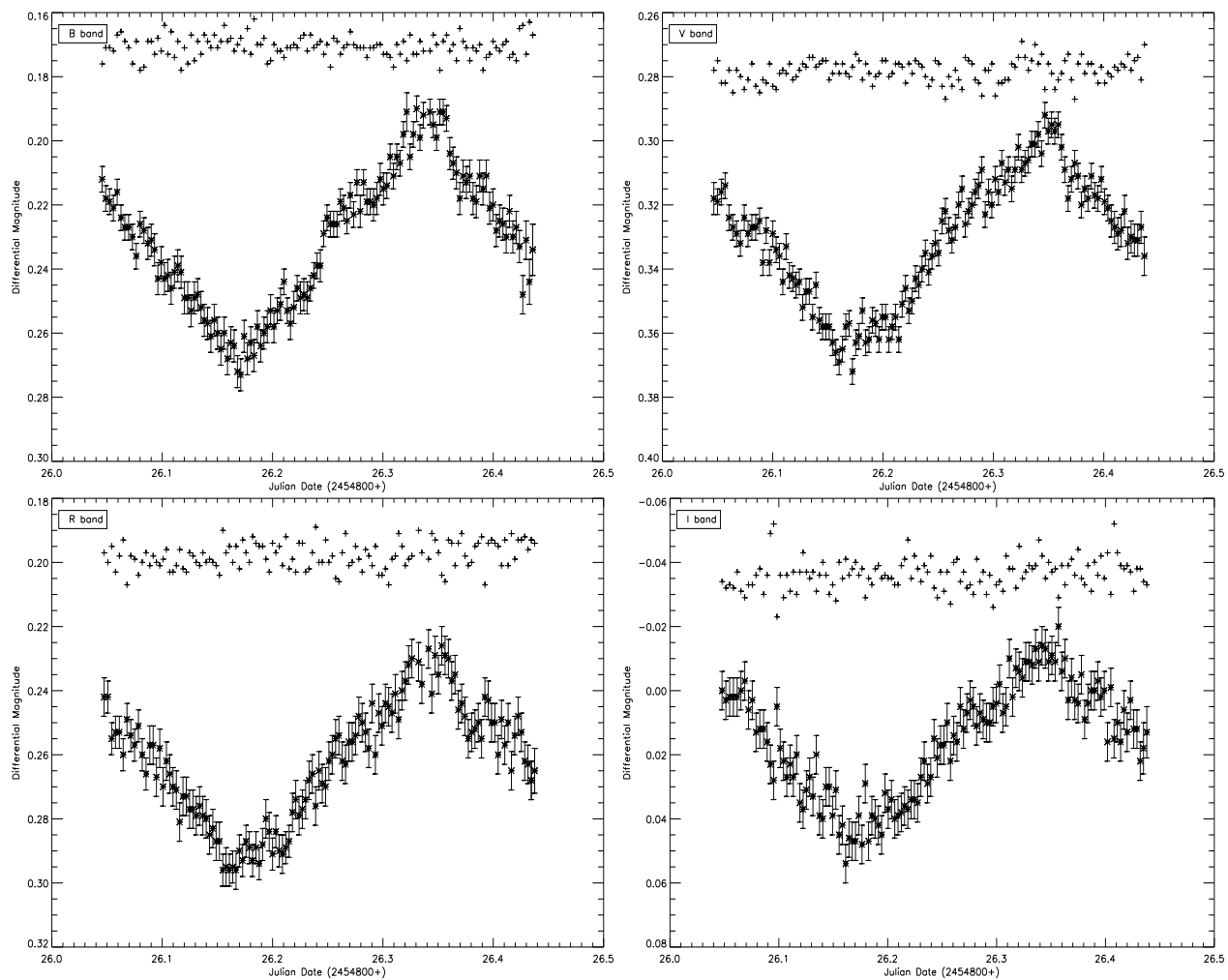


Fig. 8.— Intranight differential light curves on JD 2454826 in B (top left), V (top right), R (bottom left) and I (bottom right) bands. Crosses represent the differential magnitude between the source and star 5 while plus signs represent the differential magnitude between star 5 and star 6.

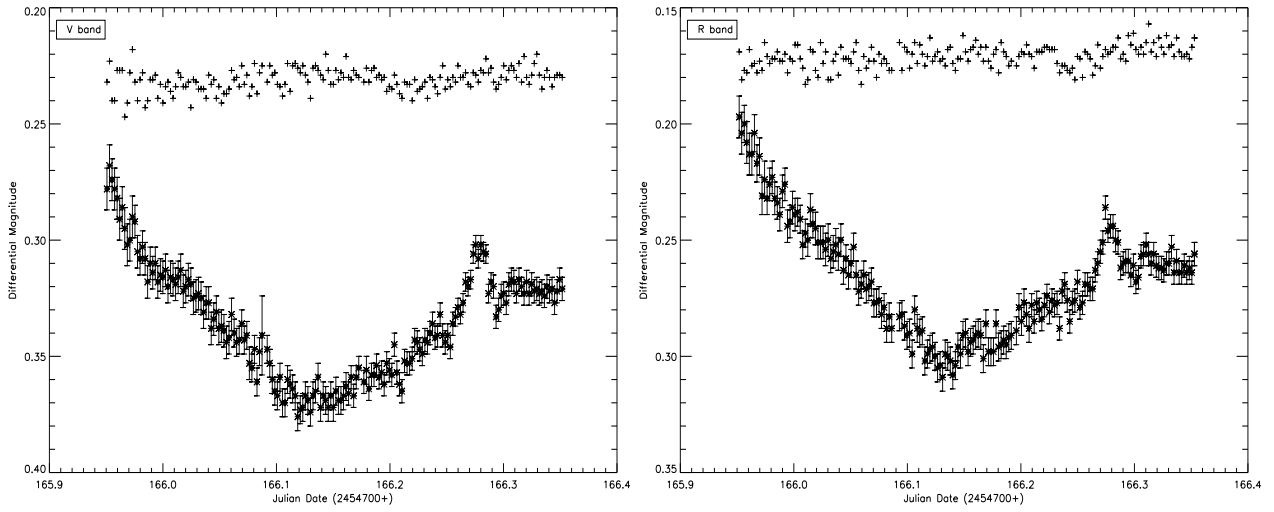


Fig. 9.— Intranight differential light curves on JD 2454865 - 2454866 in V (left) and R (right) bands. Crosses represent the differential magnitude between the source and star 5 while plus signs represent the differential magnitude between star 5 and star 6.

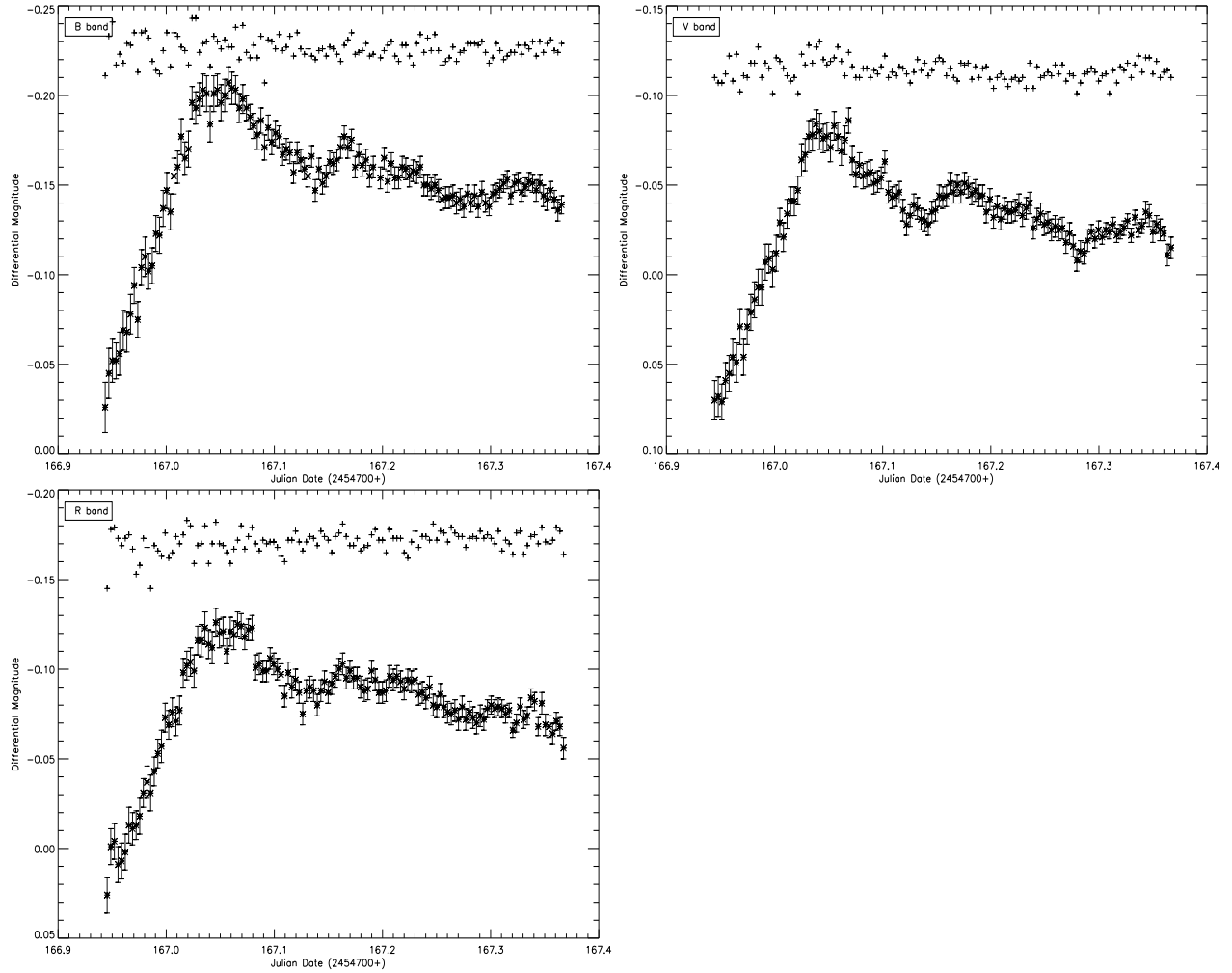


Fig. 10.— Intranight differential light curves on JD 2454866 - JD 2454867 in B (top left), V (top right) and R (bottom left) bands. Crosses represent the differential magnitude between the source and star 5 while plus signs represent the differential magnitude between star 5 and star 6.

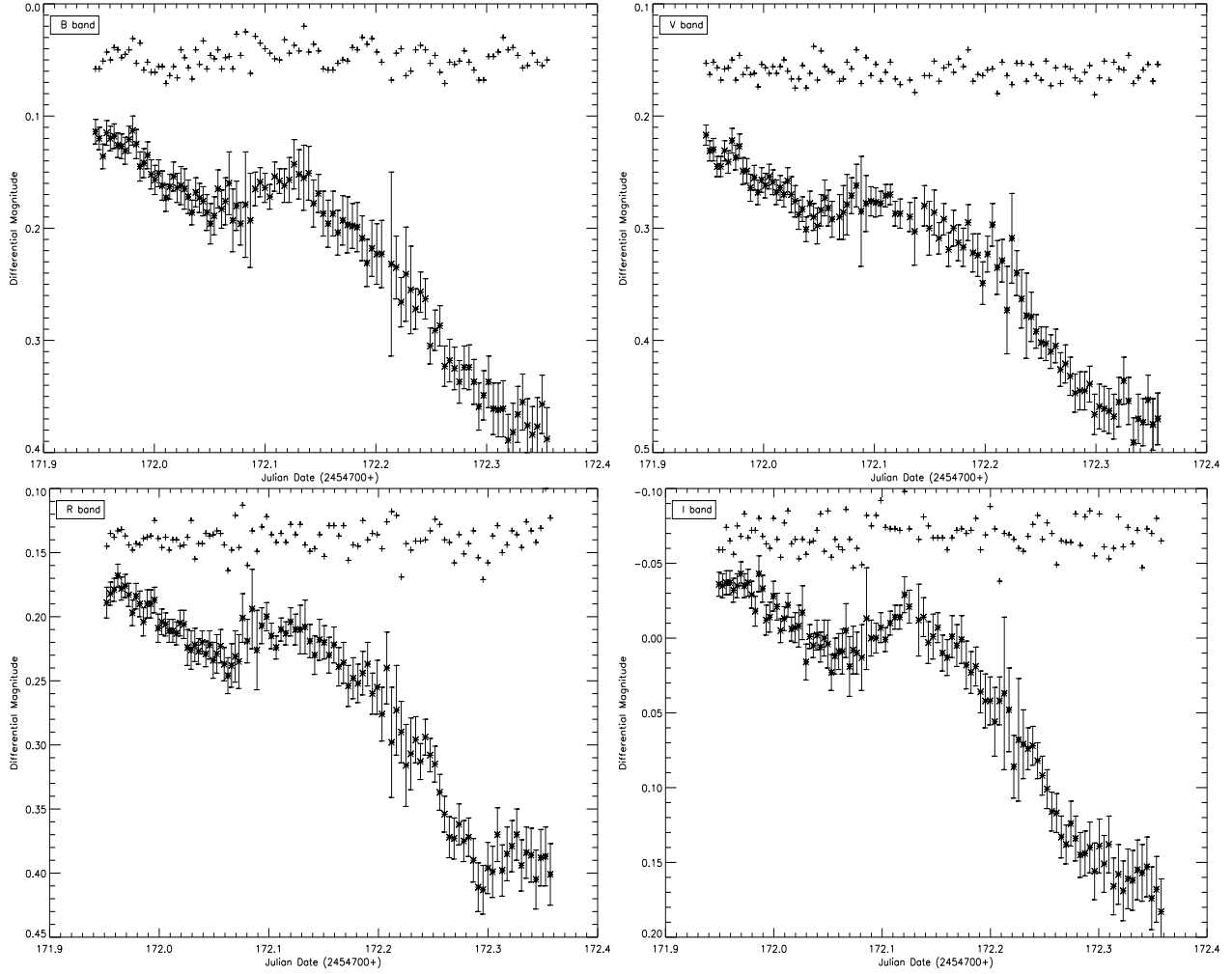


Fig. 11.— Intranight differential light curves on JD 2454871 - JD 2454872 in B (top left), V (top right), R (bottom left) and I (bottom right) bands. Crosses represent the differential magnitude between the source and star 5 while plus signs represent the differential magnitude between star 5 and star 6.

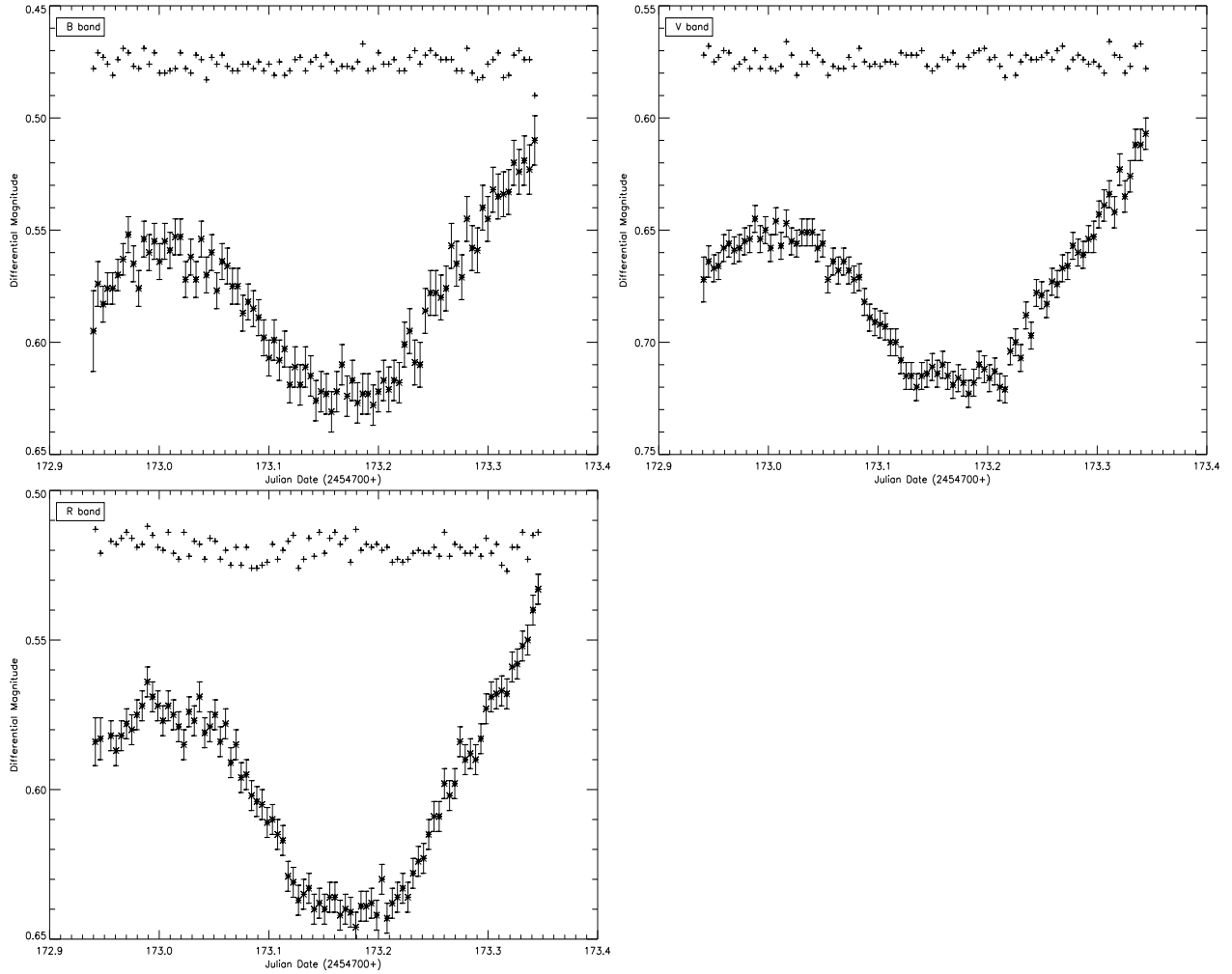


Fig. 12.— Intranight differential light curves on JD 2454872 - JD 2454873 in B (top left), V (top right) and R (bottom left) bands. Crosses represent the differential magnitude between the source and star 5 while plus signs represent the differential magnitude between star 5 and star 6.

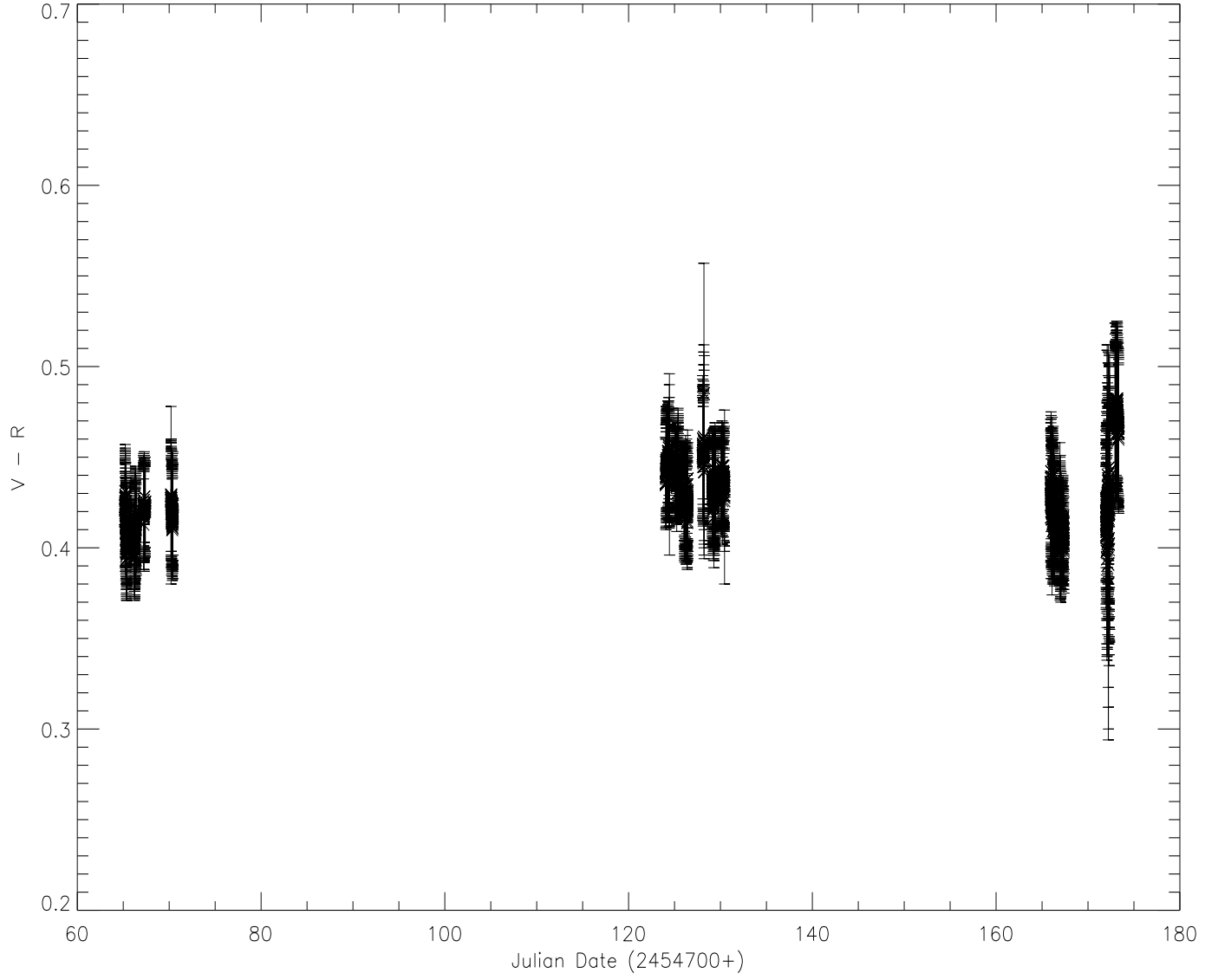


Fig. 13.— Color vs. time in the whole monitoring campaign.

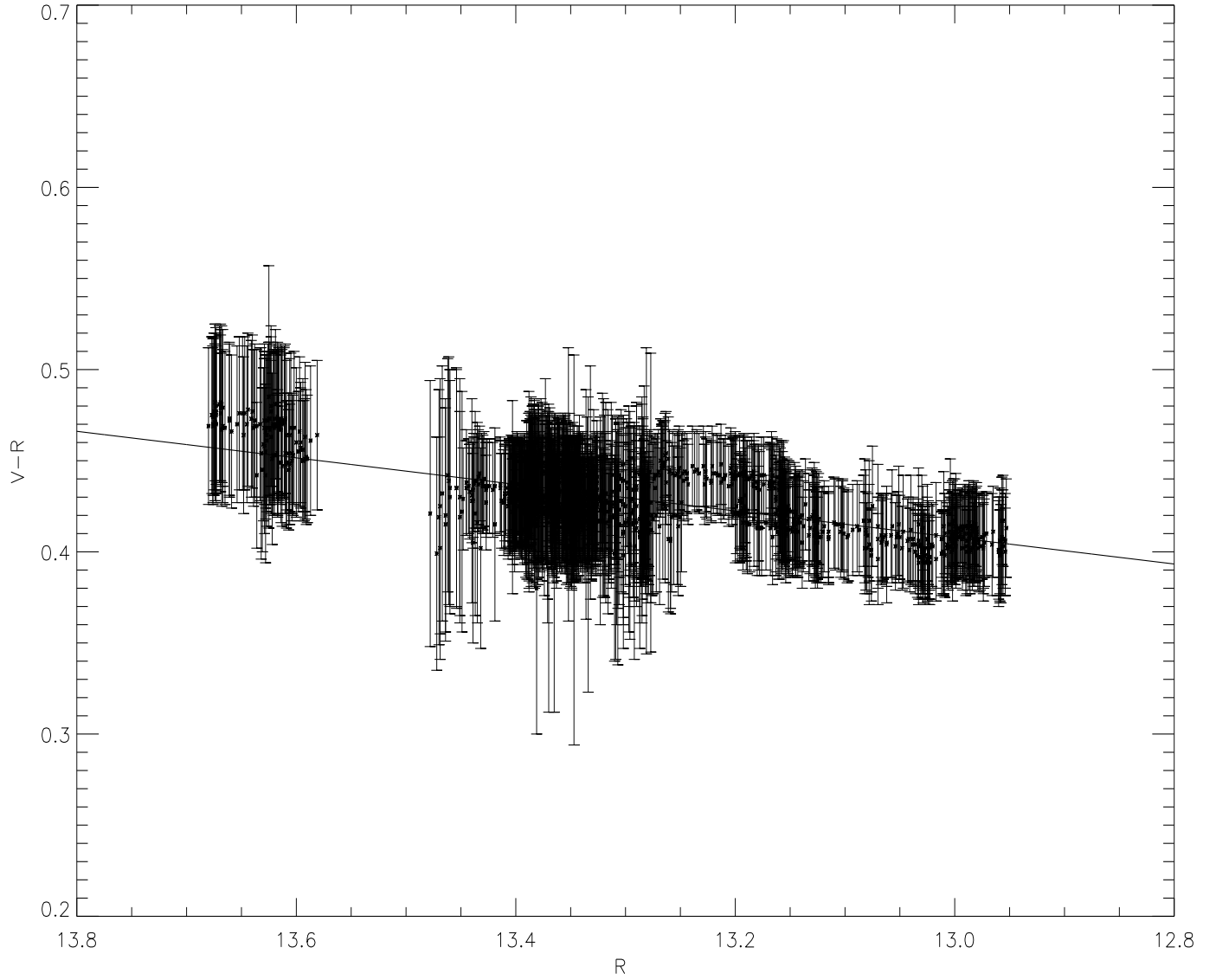


Fig. 14.— Color vs. magnitude in the whole monitoring campaign. The solid line is the linear fit to the points. The Pearson correlation coefficient is 0.753, indicating strong correlations between color and magnitude.

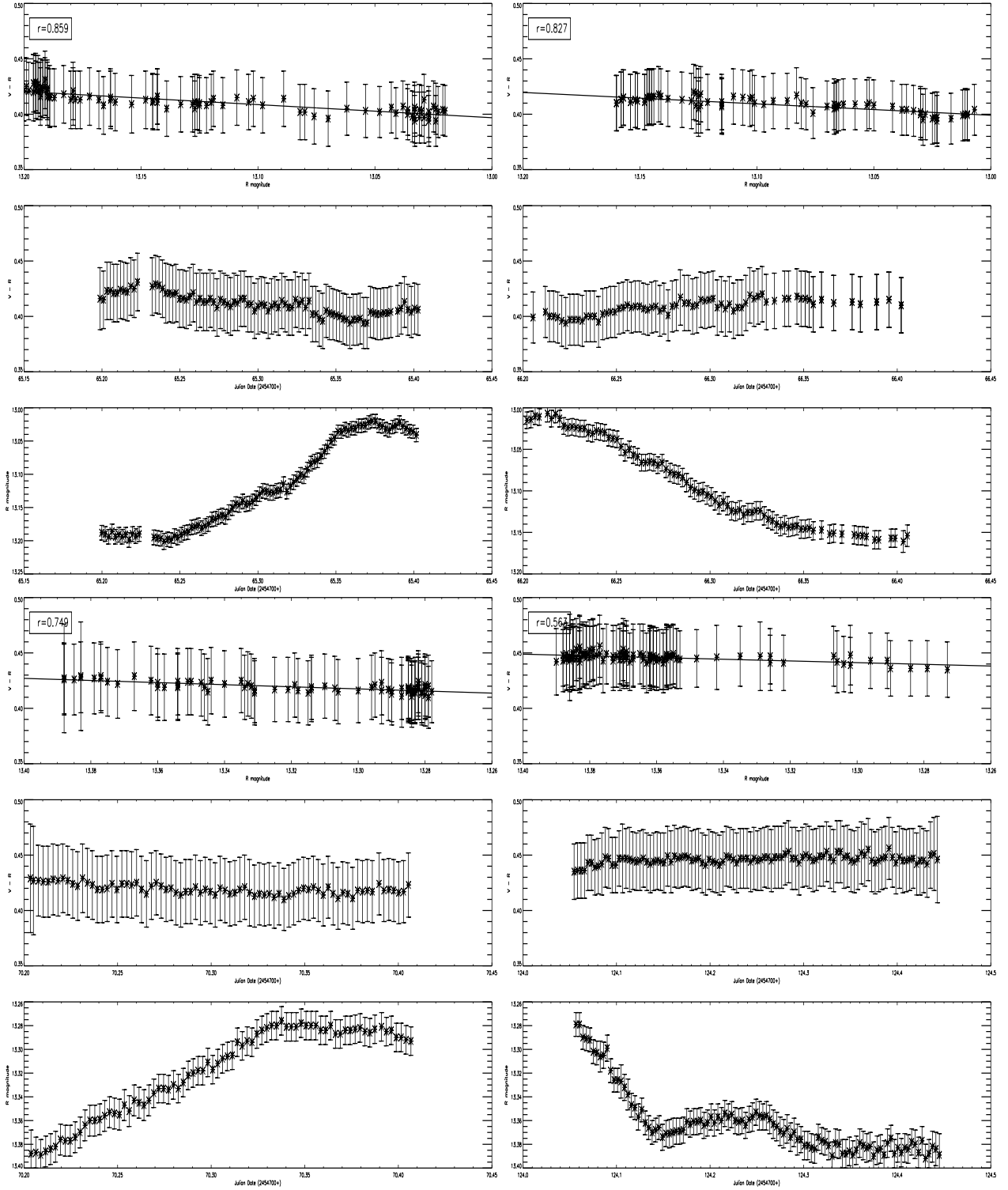


Fig. 15.— Some examples of S5 0716 + 714 showing the relationship between the $V - R$ color index vs source brightness (top panel), color index vs time (middle panel) and the corresponding brightness change with time (bottom panel). Solid lines are the best fit to the data points. r indicates the linear Pearson correlation coefficient of the best fit. Date of observations are 25 10 2008 (top left), 26 10 2008 (top right), 30 10 2008 (bottom left),

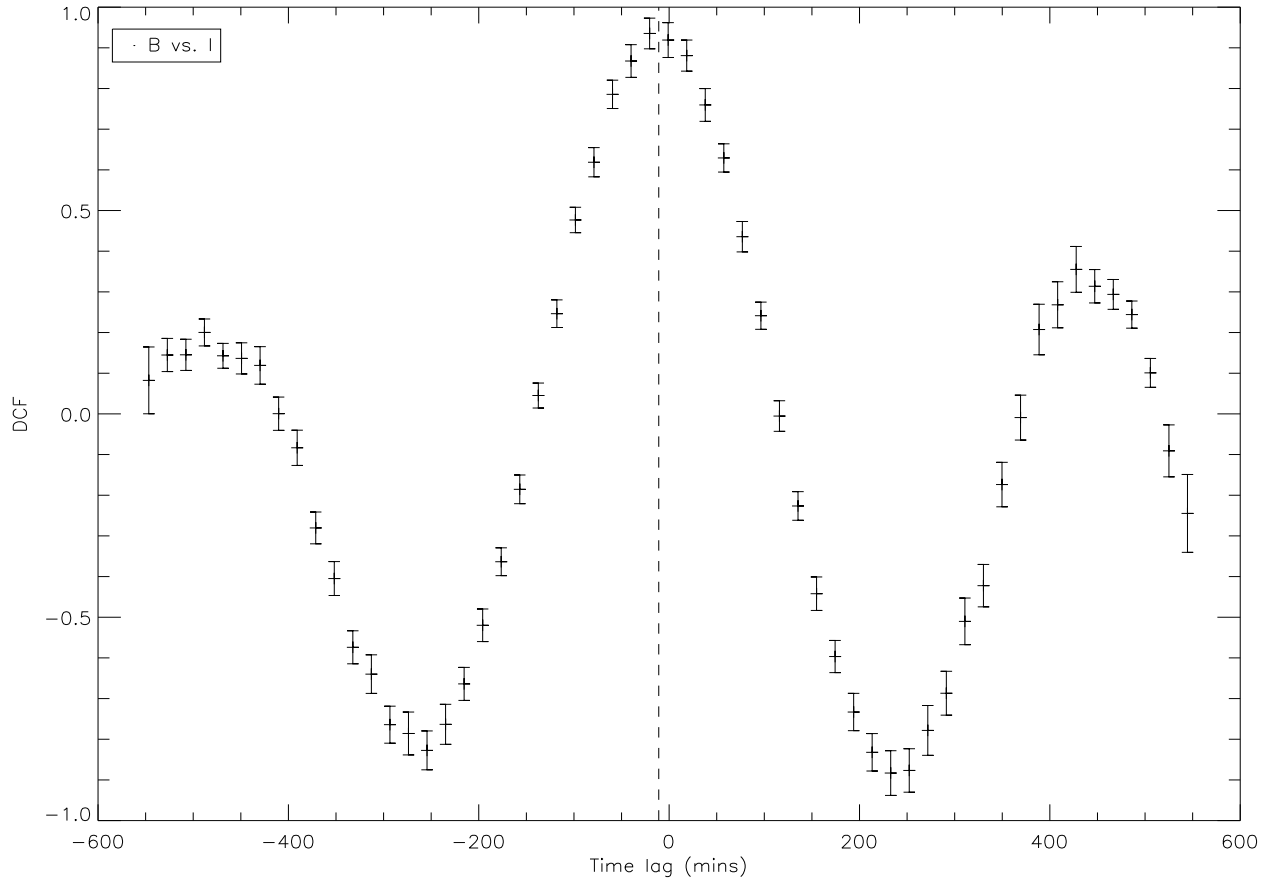


Fig. 16.— Discrete correlation functions between B and I bands. The dashed line indicates the centroid.

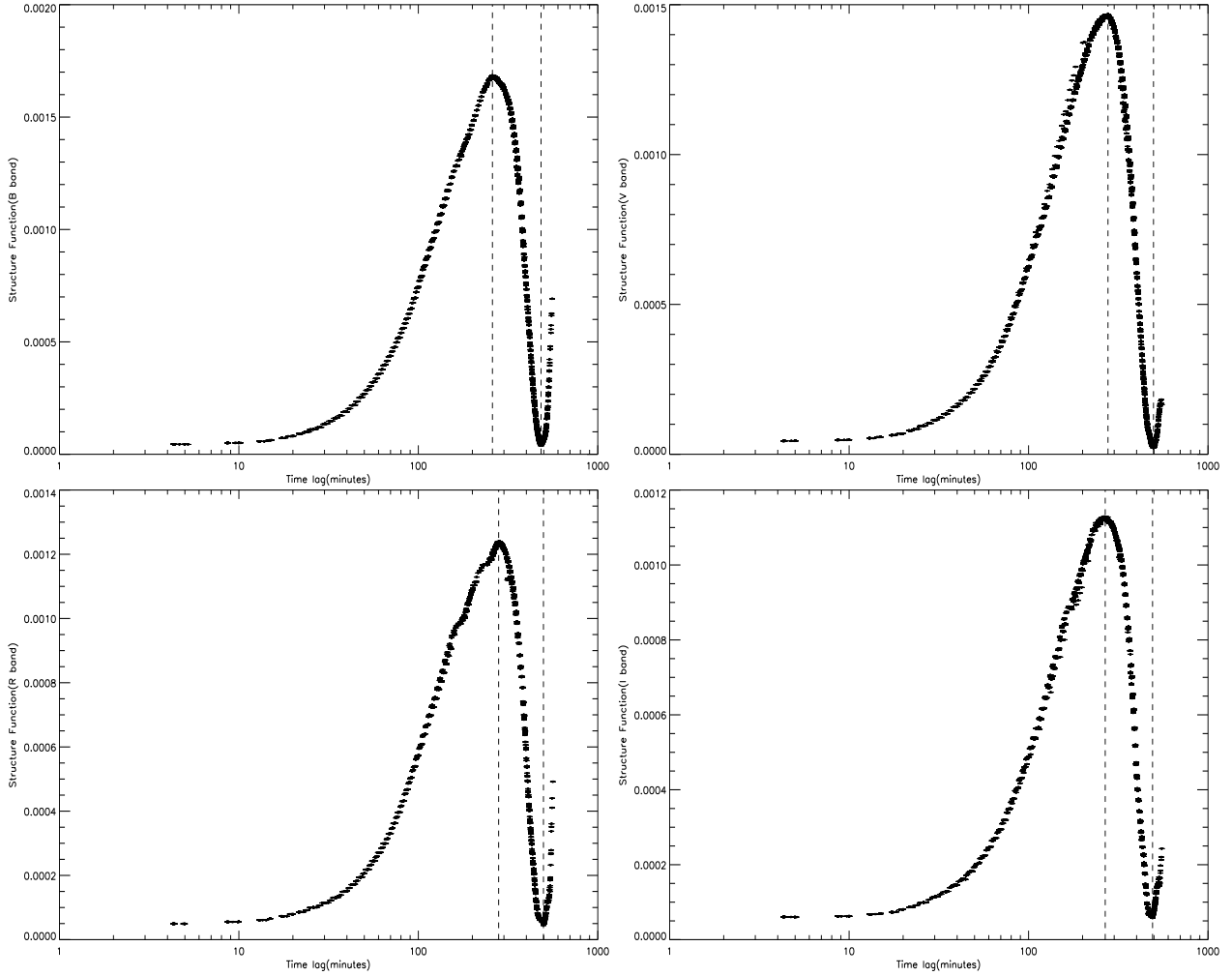


Fig. 17.— Structure function of S5 0716+714 on JD 2454826 in B (top left), V (top right), R (bottom left) and I (bottom right) bands. The dashed lines indicate timescales at the maxima and periods at the minima of the structure function.